Pet. Sci. (2016) 13:1–17
DOI 10.1007/s12182-016-0076-7

ORIGINAL PAPER

Genetic mechanisms of secondary pore development zones of Es_4^x in the north zone of the Minfeng Sag in the Dongying Depression, East China

Yan-Zhong Wang[1] · Ying-Chang Cao[1] · Shao-Min Zhang[1] · Fu-Lai Li[1] · Fan-Chao Meng[1]

Received: 27 October 2014 / Published online: 22 January 2016

Abstract The genetic mechanisms of the secondary pore development zones in the lower part of the fourth member of the Shahejie Formation (Es_4^x) were studied based on core observations, petrographic analysis, fluid inclusion analysis, and petrophysical measurements along with knowledge of the tectonic evolution history, organic matter thermal evolution, and hydrocarbon accumulation history. Two secondary pore development zones exist in Es_4^x, the depths of which range from 4200 to 4500 m and from 4700 to 4900 m, respectively. The reservoirs in these zones mainly consist of conglomerate in the middle fan braided channels of nearshore subaqueous fans, and the secondary pores in these reservoirs primarily originated from the dissolution of feldspars and carbonate cements. The reservoirs experienced "alkaline–acidic–alkaline–acidic–weak acidic", "normal pressure–overpressure–normal pressure", and "formation temperature increasing–decreasing–increasing" diagenetic environments. The diagenetic evolution sequences were "compaction/gypsum cementation/halite cementation/pyrite cementation/siderite cementation–feldspar dissolution/quartz overgrowth–carbonate cementation/quartz dissolution/feldspar overgrowth–carbonate dissolution/feldspar dissolution/quartz overgrowth–pyrite cementation and asphalt filling". Many secondary pores (fewer than the number of primary pores) were formed by feldspar dissolution during early acidic geochemical systems with organic acid when the burial depth of the reservoirs was relatively shallow. Subsequently, the pore spaces were slightly changed because of protection from early hydrocarbon charging and fluid overpressure during deep burial. Finally, the present secondary pore development zones were formed when many primary pores were filled by asphalt and pyrite from oil cracking in deeply buried paleoreservoirs.

Keywords Secondary pore development zone · Genetic mechanism · Diagenetic evolution sequences · Secondary pores · Dongying depression

1 Introduction

As the degree of hydrocarbon exploration in middle-shallow formations continues to improve, deeply buried formations are gradually becoming important targets for hydrocarbon exploration (Hu et al., 2013; Sun et al. 2013, 2015). Studies of anomalously high porosity and permeability in deeply buried sandstone reservoirs by Bloch et al. (2002) showed that deep formations can still develop abnormally high porosity zones that can form oil and gas fields with commercial value (Bloch et al. 2002). Understanding the genesis of deep, abnormally high porosity zones (AHPZs) is important for precisely predicting deeply buried high-quality reservoirs. This issue has been studied many times. Although the controlling factors of the formation of deep, abnormally high porosity zones vary in different regions, most geologists generally believe that mineral dissolution, shallow fluid overpressure, early hydrocarbon charging, and grain rims are the main factors that control the development of deep AHPZs (Bloch et al. 2002; Ehrenberg 1993; Warren and Pulham 2001; Meng et al. 2011, 2010; Taylor et al. 2010; Wilkinson and

✉ Yan-Zhong Wang
wangyanzhong1980@163.com

[1] School of Geosciences, China University of Petroleum, Qingdao 266580, Shandong, China

Edited by Jie Hao

Haszeldine 2011; Cao et al. 2014; Yuan et al. 2015; Ajdukiewicz and Larese 2012; Wang et al. 2014; Jiang et al. 2009).

Secondary pore development zones (SPDZ) are a typical type of abnormally high porosity zone. Since Schmidt and McDonald (1977) proposed the theory that secondary pores in clastic reservoirs can form during diagenetic processes (Schmidt and McDonald 1977), scientists worldwide have made significant progress in identifying the distinguishing features, genetic mechanisms, distribution, and geological significance of secondary pores (Schmidt and McDonald 1979; Giles and De Boer 1990; Osborne and Swarbrick 1999; Higgs 2007; Zhu et al. 2006; Zhang 2007; Zeng 2001; Yuan and Wang 2001; Liu and Zhu 2006; Wang et al. 1995; Wang and Zhao 2001; Ma et al. 2005; Zhang et al. 2008; Dutton and Loucks 2010; Taylor et al. 2015). Currently, SPDZs in shallow layers, which correspond to the mature stage of organic matter evolution, are considered to be generated from the dissolution of aluminum silicates and carbonate minerals by organic acids and CO_2 from organic matter evolution (Zeng 2001; Yuan and Wang 2001; Liu and Zhu 2006; Wang et al. 1995; Zhang et al. 2014). However, different viewpoints exist regarding the generation of deep SPDZs. Some authors believe that these features form by mineral dissolution in low porosity reservoirs at deep burial depths (Yuan and Wang 2001). Other authors, however, believe that the large amounts of secondary pores that form in these shallow formations are effectively preserved during deep burial, while primary pores are destroyed, which results in the formation of deep SPDZs (Wang et al., 2001; Ma et al. 2005; Zhang et al. 2008; Bjørlykke and Jahren 2012; Bjørlykke 2014).

Petroleum exploration in the deeply buried nearshore subaqueous fans in the Es_4^x sub-member in the Minfeng Sag, Dongying Depression, has greatly improved in recent years. For example, the daily oil production from depths of 4316.6–4343 m in the Fengshen1 well in Es_4^x is 81.7 t, and the daily gas production is 118,336 m^3. The reservoirs in the nearshore subaqueous fans, which are closely related to gypsum layers and the source rocks, experienced a complex burial evolution, including tectonic subsidence—uplift—subsidence and an alternating acidic-alkaline diagenetic environment. The current reservoir space mainly consists of secondary pores, and primary pores have been mostly destroyed. Exploration of the Dongying Depression shows that four sets of source rocks exist in the Es_4^x, Es_4^s, Es_3^x, and Es_3^z sub-members and that the total thickness of these source rocks exceeds 2000 m.

The reservoirs in the Es_4^x sub-member could potentially form abundant secondary pores during shallow burial because the organic matter in Es_4^x's source rocks could supply organic acids in a shallow open system. However, all the deep SPDZs in the Paleogene sandstones in the Dongying Depression are simply interpreted as having formed from deep burial mineral dissolution (Yuan and Wang 2001; Zhu et al. 2007). Some questions require further studies, such as whether these deep secondary pore development zones were originally shallow secondary pore development zones that were preserved effectively during deep burial and how these shallow secondary pore development zones were preserved during deep burial. These unresolved problems produce great difficulties and risks for the exploration and development of hydrocarbons in these reservoirs. For instance, the drilling of the Fengshen2 and Fengshen3 wells close to the Fengshen1 well was not successful (the former were dry wells and the latter only produced 2.64×10^4 m^3 of gas daily) (Zhong et al. 2004).

The characteristics and genetic mechanisms of the SPDZs in Es_4^x in the Minfeng Sag were systematically studied based on a combination of core observations, thin section identification, SEM observations, fluid inclusion analysis, core X-ray analysis, vitrinite reflectance tests, and core properties analysis, along with additional knowledge regarding the tectonic evolution history, thermal evolution of organic matter, and history of hydrocarbon accumulation in the study area. The results of this study show that the deep SPDZs in the study area experienced the formation of significant secondary pores at shallow depth and the occupation of many primary pores by massive asphalt and pyrite from oil cracking in deeply buried paleo-reservoirs under high temperature. This achievement is significant for re-evaluating the genetic mechanisms and distribution of deep high-quality reservoirs and the deployment of hydrocarbon exploration in deep formations.

2 Geological background

The Dongying Depression is a sub-tectonic unit that lies in the southeastern part of the Jiyang sub-basin of the Bohai Bay Basin in East China. This unit is a Meso-Cenozoic half graben rift-downwarped lacustrine basin, which developed on Paleozoic bedrock paleotopography (Yuan and Wang 2001). The Dongying Depression, which lies east of the Qingtuozi Salient, south of the Luxi Uplift and Guangrao Salient, west of the Linfanjia and Gaoqing Salients, and north of the Chenjiazhuang-Binxian Salient, covers an area of 5850 km^2 with an east–west axis of 90 km and a north–south axis of 65 km. Additionally, the depression is generally NE-trending. In profile view, the Dongying Depression is a half graben with a faulted northern margin and a gentle southern margin. In plan view, this depression is further subdivided into secondary structural units, such as a northern steep slope zone, a middle uplift, the Lijin, Minfeng, Niuzhuang, and Boxing sags, and a southern gentle slope zone (Zhang et al. 2006) (Fig. 1).

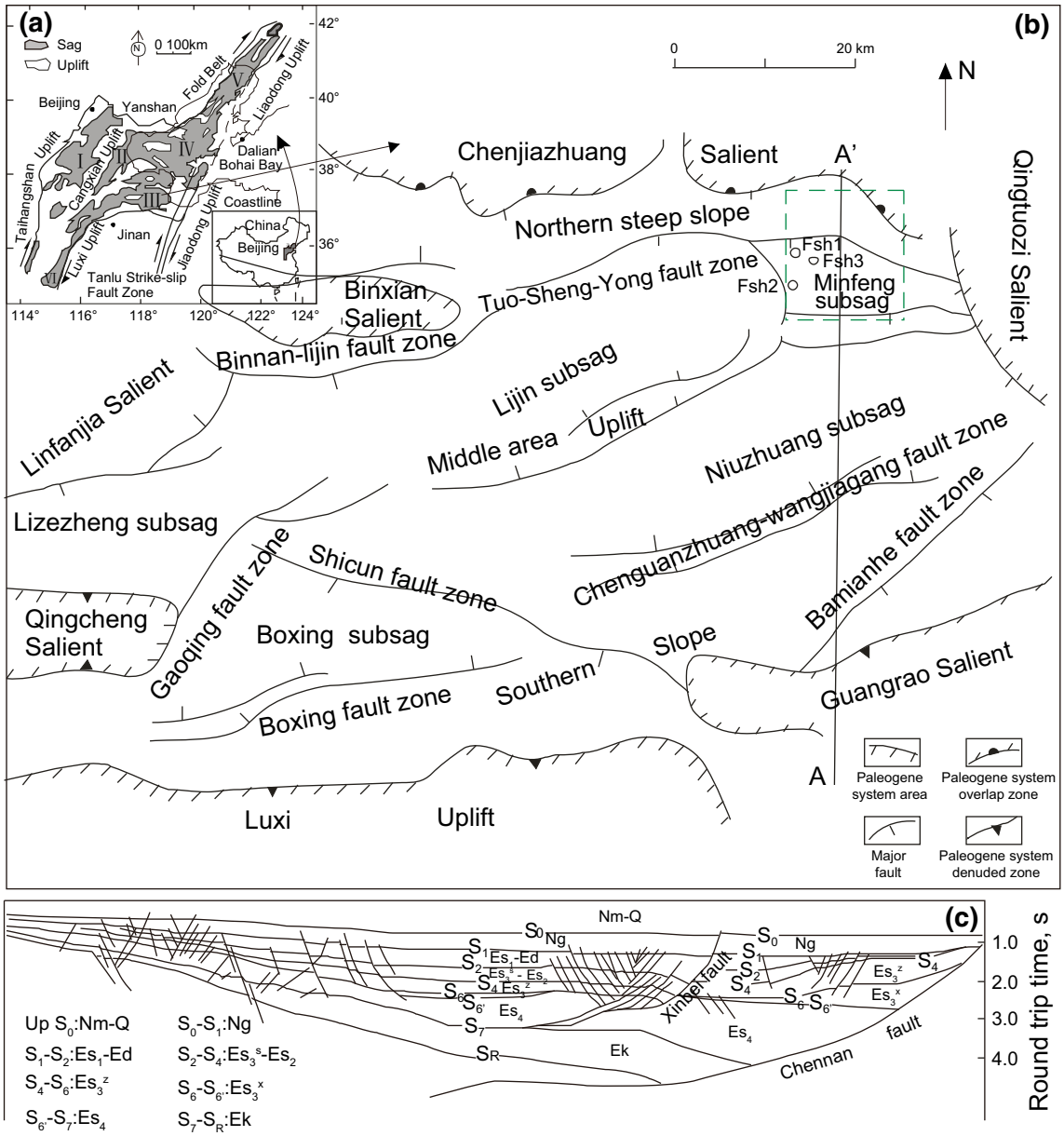

Fig. 1 **a** Tectonic setting of the Dongying Depression in the Jiyang Sub-basin (III) of the Bohai Bay Basin. Other sub-basins in the Bohai Bay Basin in East China include the Jizhong Sub-basin (I), Huanghua Sub-basin (II), Bozhong Sub-basin (IV), Liaohe Sub-basin (V), and Dongpu Sub-basin (VI) (according to Liu et al. 2012). **b** Structural map of the Dongying Depression with well locations. The area in the green line is the study area, which is located in the northern zone of the Minfeng Sag of the Dongying Depression. **c** Section of A–A′ in map (**b**). S_0, S_1, S_2, S_4, S_6, $S_{6'}$, S_7, and S_R are major seismic reflection boundaries. *Nm* Neocene Minghuazhen Formation; *Q* Quaternary Period; *Ng* Neocene Guantao Formation; *Ed* Paleogene Dongying Formation; Es_1 The first member of the Paleogene Shahejie Formation (Es); Es_2 The second member of Es; Es_3^s The upper part of the third member of Es; Es_3^z The middle part of the third member of Es; Es_3^x The lower part of the third member of Es; Es_4 The fourth member of Es; *Ek* Paleogene Kongdian Formation (Liu et al. 2012)

The Minfeng Sag lies in the northeastern area of the Dongying Depression, north of the Chenjiazhuang Salient, south of the middle uplift, east of the Qingtuozi Salient, and west of the Lijin Sag (Fig. 1). During the depositional period of the Es_4^x sub-member, the Dongying Depression in this early rift stage was characterized by an arid climate, a small lake-water area, and high salinity. The northern steep slope zone of the Minfeng Sag is a structural belt in the steep slope zone that is controlled by the Chennan boundary fault, which is located near the subsidence center with deeper water. Terrigenous clastic sediments were transported by seasonal floods to the deep lake, leading to

the deposition of the nearshore subaqueous fans in the downthrown side of the Chennan fault. These fans were distributed close to lacustrine source rocks (Sui et al. 2010). During flood stagnation, the water evaporated rapidly, and thick gypsum and halite were deposited. In vertical profile view, the strata show a sedimentary assemblage of interbedded gypsum and clastic rocks.

3 Methodology and database

This study used cast thin sections and SEM observations to analyze the characteristics of the reservoir spaces based on effective reservoir porosity cutoffs. Porosity data were combined with porosity cutoffs to determine the distribution of SPDZs. The sedimentary characteristics, secondary pore features, and diagenetic evolution sequences of the reservoirs in these SPDZs were studied based on the identification of these zones. The genetic mechanism and evolutionary model of the secondary pore development zones, the evolution of the diagenetic environment, and the reservoir reconstruction process were discussed.

The database that was used in the study includes approximately 250-m cores from eight wells, porosity data from 172 samples, 70 thin sections, 30 cast thin sections, six SEM samples, and 80 fluid inclusion samples. The core samples were provided by the Geological Scientific Research Institute of the Sinopec Shengli Oilfield Company. The porosity was tested by a 3020-62 helium porosity analyzer at the Exploration and Development Research Institute of the Sinopec Zhongyuan Oilfield Company. The SEM samples were examined with a Quanta200 SEM with an EDAX energy dispersive X-ray spectrometer at the Geological Scientific Research Institute of the Sinopec Shengli Oilfield Company. The thin sections were made by the CNPC Key Laboratory of Oil and Gas Reservoirs at the China University of Petroleum and were examined by the authors with an Axio Scope A1 APOL digital polarizing microscope, which was produced by the German company Zeiss. The fluid inclusions were analyzed using a THMSG600 conventional inclusion temperature measurement system, which was produced by the British Company Linkam.

4 Results

4.1 Distribution of SPDZs

The term "secondary pore development zone" has been generally applied by scientists around the world but has not been defined precisely and scientifically. Most geologists suggest that an SPDZ is the depth interval for which the real porosity evolution curve is higher than the normal porosity evolution curve and the percent of secondary pores is over 50 % (Liu and Zhu 2006; Zhu et al. 2007; Shi et al. 2005; Zhong et al. 2003; Zhang et al. 2003; Zheng and Wu 1996). However, the porosity values of reservoirs in secondary pore development zones and the methods that are used to determine the normal porosity evolution curve have not been clearly explained. Additionally, the methods that are used to determine the real porosity evolution curve have not yet been unified. For example, one method that is used to determine this curve is to fit the functional relationship between the porosity and depth (Liu and Zhu 2006; Zhu et al. 2007; Zhong et al. 2003; Zhang et al. 2003). Another method uses the porosity envelope curve of the porosity-depth profile as the real porosity evolution curve (Yuan and Wang 2001; Zhu et al. 2010; Liu et al. 2010). In this paper, an SPDZ is first defined as a zone where high porosity reservoirs with more than 50 % secondary pores develop. This definition includes three meanings: (1) the percent of secondary pores is greater than 50 %; (2) the porosity of the reservoirs is higher than the effective reservoir porosity cutoff because the absolute content of secondary pores is high; (3) high porosity reservoirs concentrate to form belts at a particular depth interval in the porosity-depth profile, with the porosity envelope curve bulging towards higher porosities.

The effective reservoir porosity cutoff is the basis for determining SPDZs. Only when the effective porosity cutoff is known, can the development of high porosity reservoirs be confirmed and the distribution of secondary pore development zones determined. Based on collections and arrangements of a large number of porosity and permeability data and the interpretation of oil, gas, water layers, and dry layers, the quantitative functional relationship between the effective porosity cutoff and burial depth from the Es_3^z to Es_4^x sub-members in the northern zone of the Minfeng Sag was obtained using the oil test method, which was developed by Wang (2010):

$$\varphi_{\text{cutoff}} = -8.1623\ln(H) + 73.765 \quad R^2 = 0.8833$$

φ_{cutoff}: porosity cutoff, %; H: burial depth, m.

Using point-counting methods, a quantitative analysis of various pores in cast thin sections shows that the percentage of secondary pores in the reservoirs in the nearshore subaqueous fans in the Es_4^x sub-member is greater than 50 % (Fig. 2). Overlapping the φ_{cutoff} curve and the porosity envelope curve in the porosity-depth profile shows that two secondary pore development zones, whose depths range from 4200 to 4500 m and from 4700 to 4900 m, developed in the Es_4^x sub-member in the northern zone of the Minfeng Sag.

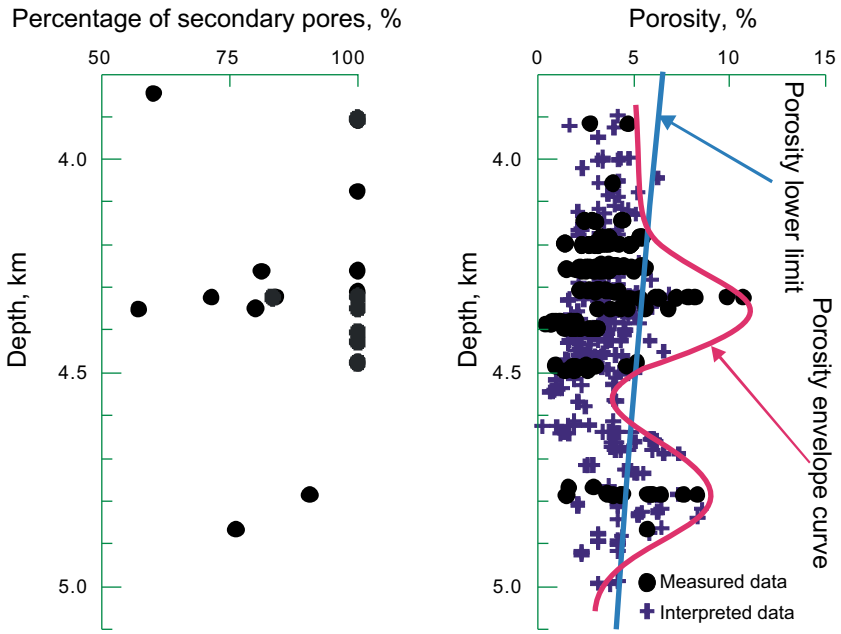

Fig. 2 By overlapping the effective reservoir porosity cutoff in the porosity-depth profile, the relationship between the porosity envelope curve and the porosity lower limit shows two secondary pore development zones, which range from 4200 to 4500 m and from 4700 to 4900 m, in Es_4^x in the northern zone of the Minfeng Sag

4.2 Reservoir characteristics in secondary pore development zones

4.2.1 Sedimentary characteristics

Multi-phase nearshore subaqueous fans developed in the Es_4^x sub-member in the northern zone of the Minfeng Sag. The nearshore subaqueous fans can be subdivided into inner fan, middle fan, and outer fan sub-facies according to the sedimentary features and hydrodynamic conditions. The inner fan sub-facies are dominated by major channels that are mainly filled with thick matrix-supported conglomerates and lack normal lacustrine mudstones between multi-phase fans. The poorly sorted conglomerates have a high proportion of matrix, with sub-angular grains floating among them, and scoured bases can be identified, which indicates proximal and rapid accumulation. The middle fans are dominated by braided channels and inter-distributaries. The lithology of the braided channels mainly consists of massive gravel sandstones and superimposed coarse sandstones with scoured bases, which have grain-supporting characteristics, medium-poor sorting, moderate thickness, and low matrix content. Normally graded bedding, scouring structure, and intensely contemporaneous deformation structures are present. The inter-distributaries are typical turbidites, which contain thin and fine-grained sediments with high matrix content. Lacustrine mudstones are generally deposited among multi-stage middle fans (Fig. 3). The lithology of the outer fan sub-facies includes typical turbidites, which mainly consist of dark-gray mudstones with thin interbedded sandstones and pebbly sandstones (Fig. 3).

The relationship between different micro-facies in the nearshore subaqueous fans and their physical properties were identified based on sedimentary analyses of individual wells. This relationship shows that the high porosity reservoirs in the SPDZs are located in the center of thick sand beds that were deposited in braided channels in the middle fan, in contrast to the reservoirs in the inner and outer fans or the inter-distributaries in the middle fan. The low porosity reservoirs that correspond to the SPDZs include thin sand bodies in the outer fan, inter-distributaries in the middle fan, marginal reservoirs in thick sand beds in the middle fan, and thick conglomerates in the inner fan (Fig. 3).

4.2.2 Secondary pores

The secondary pores in the SPDZ reservoirs in the Es_4^x sub-member include pores that formed from the dissolution of feldspars and acid extrusive rock debris, detrital quartz grains and quartz overgrowths, carbonate and pyrite cements and compacted cracks in feldspars and other brittle grains. These secondary pores originated from the dissolution of feldspars and rock debris. They mainly occur as intra-granular pores and grain boundary pores (Appendix Fig. 7A, B, C). The quartz grains and quartz overgrowths usually dissolved along the boundaries, which formed irregular pores (Appendix Fig. 7D). Euhedral ankerite

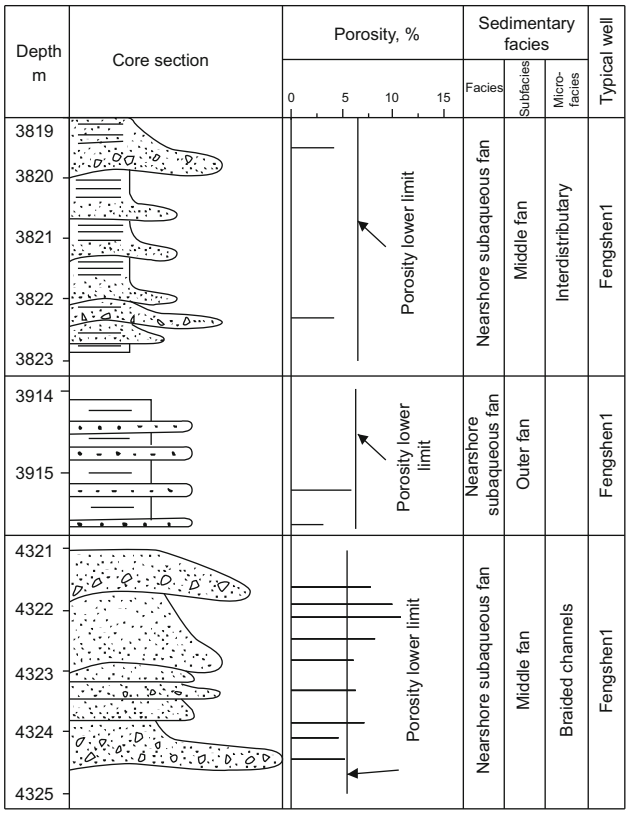

Fig. 3 Sedimentary characteristics and physical properties of the reservoirs in the Es_4^x sub-member in the northern zone of the Minfeng Sag. The effective reservoirs are the conglomerate in the central part of the positive sedimentary cycle of braided channels in the middle fan of the nearshore subaqueous fans

cement dissolved along its boundaries, while dolomite cement dissolved to form secondary pores in cements (Appendix Fig. 7E, F). Pyrite-dissolved pores are mostly found within cements (Appendix Fig. 7G). Compacted cracks in feldspars, which generally cut through the grains, are wide at one end and narrow at the other side of the grains (or are irregular) (Appendix Fig. 7H). Quantitative data regarding the amounts of different types of secondary pores in cast thin sections show that feldspar-dissolved pores and carbonate-dissolved pores dominate in the reservoirs in the SPDZs in the Es_4^x sub-member at depths from 4200 to 4500 m and from 4700 to 4900 m, followed by quartz-dissolved pores, a few acid extrusive rock debris-dissolved pores, pyrite-dissolved pores, and compacted cracks (Table 1).

4.2.3 Diagenetic evolution sequence

The diagenesis processes that occurred in the Es_4^x reservoirs in the SPDZs include the multi-stage dissolution of minerals (e.g., feldspar, carbonate, and quartz), multi-stage cementation (e.g., carbonate, silica, anhydrite, pyrite, and asphalt), and complex replacement (Appendices 1, 2, 3).

Table 1 Types and percentages of secondary pores in Es_4^x's secondary pore development zones in the northern zone of the Minfeng Sag

Secondary pore development zone Types of secondary pores	4200–4500 m	4700–4900 m
Feldspar-dissolved pores, %	25–70/48.6	62.5–72.9/67.7
Carbonate-dissolved pores, %	12.7–69.0/40.4	10.4–15.6/13.0
Rock debris-dissolved pores, %	0–6.33/1.58	0–6.25/3.13
Quartz-dissolved pores, %	0–12.5/4.7	6.25–15.6/10.9
Pyrite-dissolved pores, %	0–12.5/3.13	0–6.25/3.13
Cracks, %	0–6.33/1.58	0–4.17/2.08

Note: "25-70/48.6" means "Minimum–Maximum/Average"

The diagenetic evolution sequences of the reservoirs in the SPDZs were established based on an analysis of the types and features of the diagenesis, including the texture of authigenic minerals, the metasomatism-crosscutting relationship, the dissolution-filling relationship, and the homogenization temperatures of fluid inclusions.

The siderite cements are mainly granular and lumpy and are products of early diagenesis (Appendix Fig. 8A). The halite is completely crystalline (Appendix Fig. 8B), and the anhydrite was replaced by dolomite or ankerite, which suggests that the halite and gypsum were early cements, with gypsum turning into anhydrite after dehydration at high temperatures. Quartz overgrowths were replaced by ankerite and pyrite, which demonstrates that the quartz overgrowths formed earlier than the ankerite and pyrite (Appendix Fig. 8D, E). Multi-stage quartz overgrowths can be identified in thin sections. The homogenization temperature (Th) of the aqueous inclusions in the early stage of quartz overgrowths in Es_4^x is only 115 °C (Table 2). The combination of Th with burial and thermal history of the Fengshen8 well suggests the precipitation of the quartz cements at 42 Ma. The homogenization temperature of the late stage quartz overgrowths reached 155–160 °C (Table 2), which suggests that the quartz overgrowths occurred later. Ankerite was identified in the secondary pores in the feldspar grains (Appendix Fig. 8F) and carbonate cements (Appendix Fig. 7E, F), which indicates that the reservoir experienced two stages of acidic dissolution: an early stage of feldspar dissolution and a late stage of carbonate cement dissolution.

In an acidic geochemical environment, SiO_2 (aq) that is released from feldspar dissolution can precipitate in the form of quartz overgrowths. In this study, the homogenization temperatures of the oil inclusions in the quartz overgrowths and the fillings of the feldspar-dissolved pores

Table 2 Homogenization temperatures of fluid inclusions from reservoirs in Es_4^x in the northern zone of the Minfeng Sag

Well number	Depth, m	Horizon	Host minerals	Types	Inclusion number	Average homogenization temperature, °C
Feng8	4397.5	Es_4^x	Quartz overgrowth	Brine	6	115
Feng8	4200.7	Es_4^x	Quartz cement	Brine	5	124.1
Fengshen3	3785.6	Es_4^x	Quartz cement	Brine	8	133.9
Feng8*	4055.35	Es_4^x	Quartz overgrowth	Brine	3	143.3
Fengshen3	4867	Es_4^x	Quartz overgrowth	Brine	1	155
Fengshen3	4785.7	Es_4^x	Quartz overgrowth	Brine	1	155
Fengshen10	4260.6	Es_4^x	Quartz overgrowth	Brine	1	155.5
Fengshen3	4785.7	Es_4^x	Quartz overgrowth	Brine	1	160
Feng8*	4055.35	Es_4^x	Quartz overgrowth	Oil	3	99.1
Feng8*	4055.35	Es_4^x	Quartz overgrowth	Oil	5	112.6
Feng8*	4201.1	Es_4^x	Fillings of feldspar-dissolved pores	Oil	5	88.7
Feng8*	4055.35	Es_4^x	Fillings of feldspar-dissolved pores	Oil	9	91.9
Fengshen1*	4321.6	Es_4^x	Fillings of feldspar-dissolved pores	Oil	4	98.8
Feng8*	4201.1	Es_4^x	Fillings of feldspar-dissolved pores	Oil	4	108.1
Fengshen1*	4348.8	Es_4^x	Fillings of feldspar-dissolved pores	Oil	2	108.7
Feng8*	4055.35	Es_4^x	Fillings of feldspar-dissolved pores	Oil	4	109.6

* Means data from the Geological Scientific Research Institute of the Sinopec Shengli Oilfield Company

(such as SiO_2) mainly range from 88 °C to 110 °C, and the homogenization temperatures of paragenetic aqueous inclusions are about 115 °C, which suggest that the oil and aqueous inclusions formed simultaneously. This observation means that feldspar dissolution and early quartz overgrowth cementation occurred roughly during the same early period. Both carbonate cementation and quartz dissolution occur in an alkaline environment, so they may have formed during the same period. The replacement of feldspar overgrowths by ankerite (Appendix Fig. 8G) suggests that the ankerite formed later than the feldspar overgrowths, whereas the ankerite and feldspar overgrowths both formed in an alkaline environment, which indicates that they are probably products from the same period. Strong asphalt cementation is typical in the reservoirs in the SPDZs of Es_4^x. Many primary pores and various secondary pores (from the dissolution of feldspars, ankerite, quartz grains, and quartz overgrowths) are largely filled by asphalt (Appendix Fig. 8H, 3A, B, C, D, E, F). These textures suggest that asphalt formed very late, and many primary and secondary pores existed in the reservoirs before being filled with asphalt. For example, the thin section porosity of the asphalt in the reservoir at a depth of 4323.3 m in the Fengshen1 well is approximately 10 %, and the porosity that was filled by asphalt may be 22 % according to the relationship between the thin section porosity and core porosity. Song et al. (2009a) suggested that crude oil in the deep buried reservoirs in the Fengshen1 well started to crack into gas and asphalt during the late depositional period of the Minghuazhen Formation. Li et al. (2010a, b) proposed that the asphalt in the Fengshen1 well was a product of oil pyrolysis when temperatures exceeded 160 °C. Additionally, Li et al. (2010a, b) found that secondary pores in the feldspar grains were filled with asphalt, and tension fractures that are associated with the secondary pores were produced by overpressure from oil cracking (Appendix Fig. 8H). The above analysis shows that the asphalt formed relatively late. Before being filled with asphalt, the reservoirs should have had high porosity, which indicates that the porosities were well preserved during deep burial. Pyrite cements developed extensively in the northern zone of the Minfeng Sag. Partial cloddy pyrites are products of early cementation (Appendix Fig. 9G). Because mostly pyrite cements replaced quartz overgrowths (Appendix Fig. 8E), feldspar overgrowths, and ankerite (Appendix Fig. 9H), they should have formed during a late diagenetic stage. The textures of both the pyrite cements and asphalt suggest that they formed during the same period. During paragenesis with asphalt, pyrite is considered to be a reaction product of hydrogen sulfide (H_2S) from crude oil cracking under high temperatures and Fe^{2+} in reservoir fluids.

According to these comprehensive analyses, the diagenetic evolution sequence of the reservoirs in the SPDZs of Es_4^x is as follows: compaction/gypsum cementation/halite cementation/pyrite cementation/siderite cementation → feldspar dissolution/quartz overgrowth → carbonate cementation/quartz dissolution/feldspar overgrowth → carbonate dissolution/feldspar dissolution/quartz overgrowth → pyrite cementation and asphalt filling.

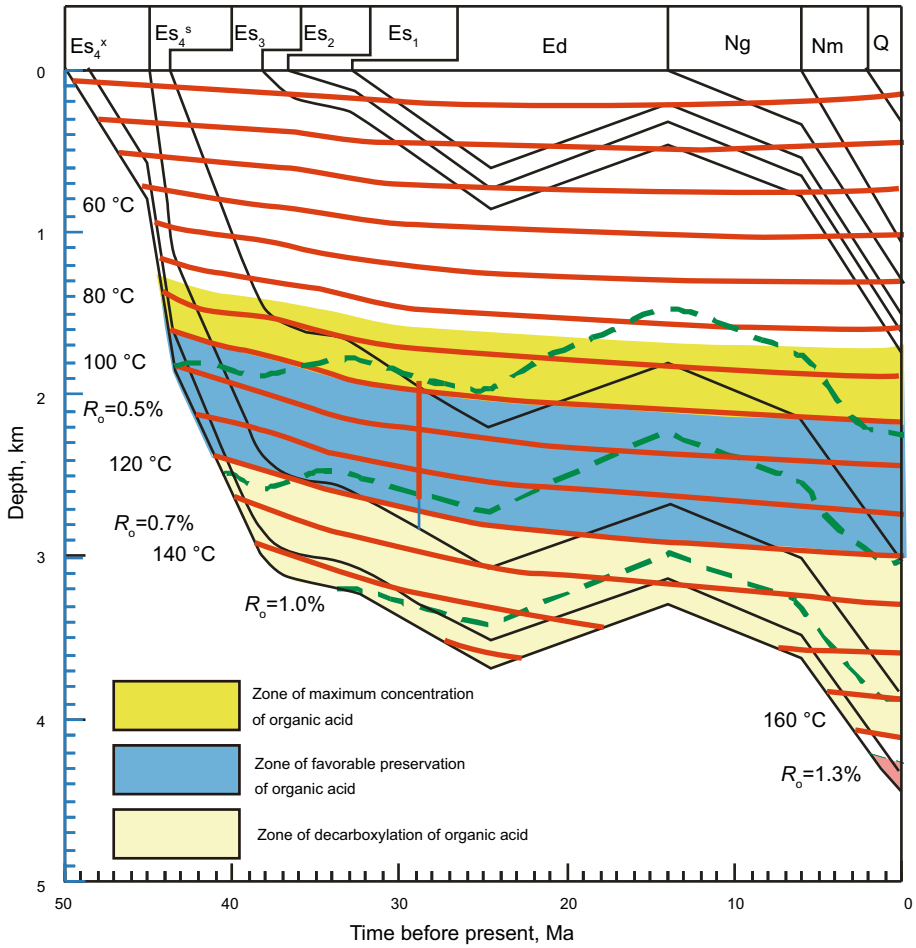

Fig. 4 The burial history and evolutionary history of organic matter from the Fengshen1 well (modified from Song et al. 2009a)

5 Discussion

Models of the diagenetic environment evolution and reservoir reconstruction were established using the burial evolution history of the Fengshen1 well based on research of the sedimentary characteristics, secondary pore features, and diagenetic evolution of the reservoirs in Es_4^x's SPDZs in the northern zone of the Minfeng Sag (Fig. 4). The genetic mechanism and evolutionary model of the SPDZs in Es_4^x are discussed from the perspective of the SPDZ at depths from 4200 m to 4500 m (Fig. 5, Fig. 6).

Gypsum-halite layers were deposited in the Es_4^x sub-member, and the thickness of the gypsum-halite layers in Es_4 is 1287.5 m in the Fengshen2 well and 267.7 m in the Fengshen1 well. Three sets of high-quality source rocks developed in Es_4 (Song et al. 2009a), and studies suggest that the gypsum-halite layer is contemporaneous with deep water source rocks. Gypsum precipitates under physico-chemical conditions with pH higher than 7.8 (Qiu and Jiang 2006), which suggests the development of an alkaline-reducing environment in the salt lake during the depositional period of the Es_4^x sub-member.

From the deposition of the Es_4^x sub-member to 44 Ma before the present (the end of the deposition of Es_4^s), the top boundary of the Es_4^x was buried to a depth shallower than 750 m at formation temperatures below 50 °C, and the bottom boundary was buried less than 1400 m at temperatures below 75 °C. The main diagenesis during this period was compaction, which led to the drainage of formation water. At this time, the salinity of the water in the pore spaces increased, which resulted in the early precipitation of gypsum and halite. Anaerobic bacteria broke down organic matter and SO_4^{2-} in the pore water, releasing organic acids, H_2S, CO_2, and other gases. Under these conditions, the Fe^{3+} in the sediments was reduced to Fe^{2+} and formed spherulitic pyrite and agglomerate siderite cement (Curtis 1978). Because the organic acids that formed during this period were mostly destroyed by bacteria, the formation water remained alkaline, and the formation exhibited normal fluid pressure. The conglomerate bodies of the nearshore subaqueous fans were similar to dome-shaped anticlines, with a flat bottom and convex top in a cross-section and was defined by Zhong et al. (2004) as "fan-anticlines" that formed by sedimentation. The inner

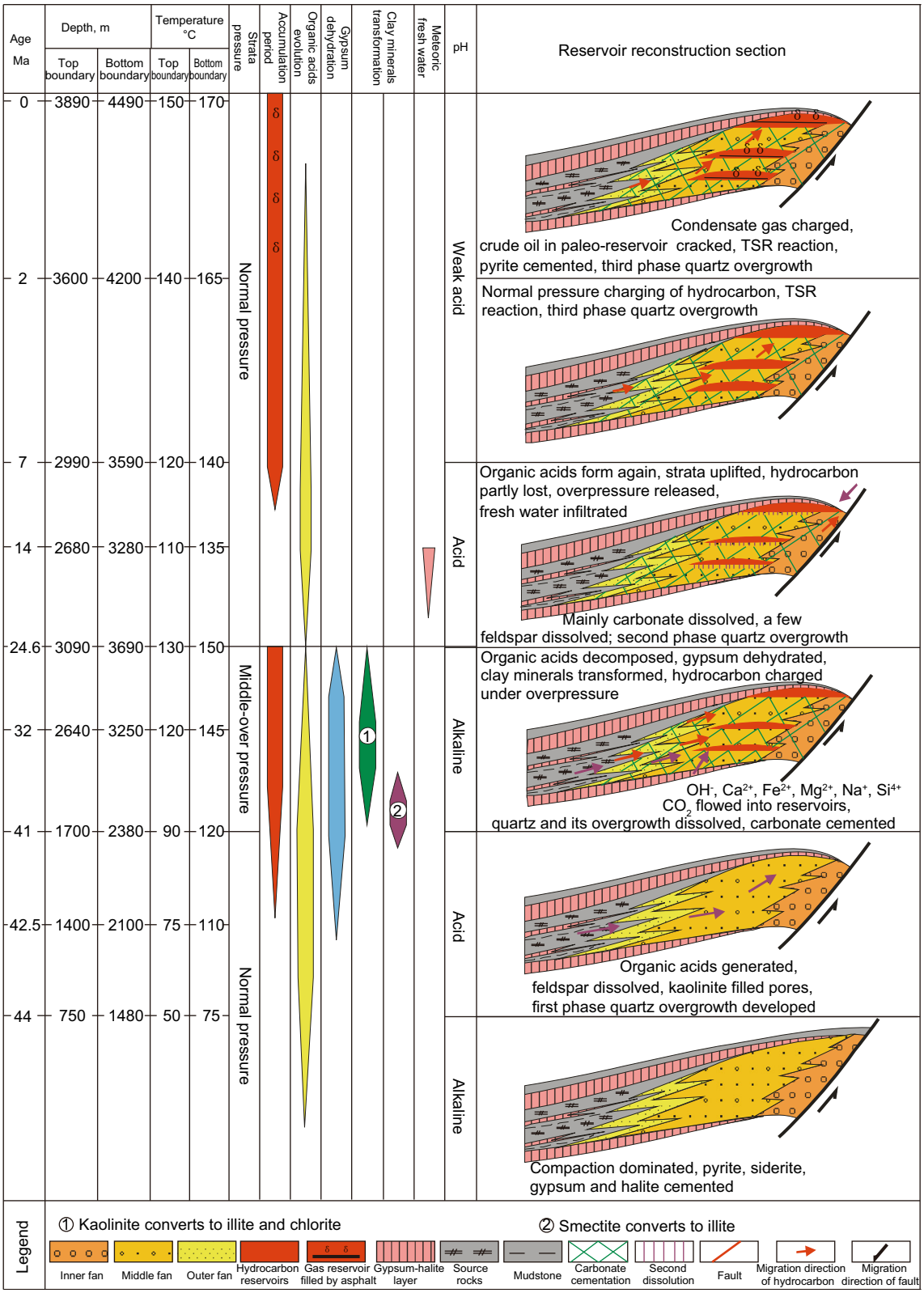

Fig. 5 Diagenetic environment evolution and reservoir reconstruction model of Es_4^x in the northern zone of the Minfeng Sag

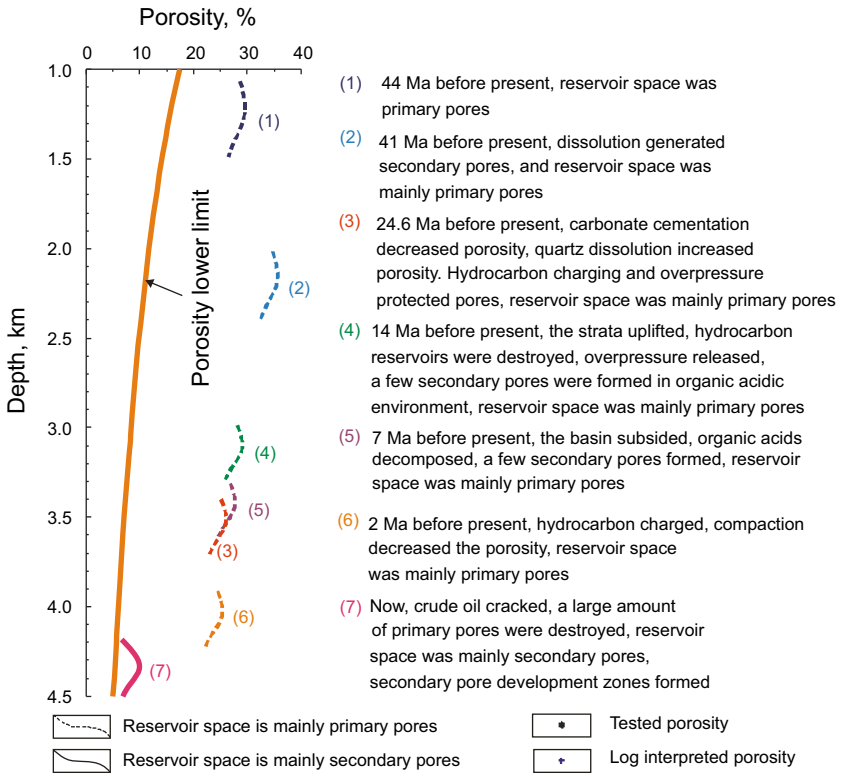

Fig. 6 Genetic mechanism and evolutionary model of $Es_4^{x\prime}$s secondary pore development zones in the northern zone of the Minfeng Sag

fans of the nearshore subaqueous fans are mainly composed of matrix-supported conglomerates, whose resistance to compaction is weak. The middle fans mainly consist of pebbly sandstones and sandstones in braided channels, whose resistance to compaction is relatively strong. The high part of the conglomerate fans had an anticlinal attitude and formed dome traps as a result of differential compaction (Wang 2003). During this period, the reservoir spaces were dominated by primary pores after compaction and early cementation (Fig. 6).

From 44 to 41 Ma before the present (the early period of the deposition of Es_3^z), the top boundary of the strata was buried at 1700 m at temperatures of 90 °C, and the bottom boundary was buried at 2380 m at temperatures of 120 °C. According to Surdam's studies (Surdam et al. 1984, 1989), significant organic acid generation occurs during burial evolution. The temperature range of the maximum concentration of short-chain carboxylic acids is 75–90 °C (a peak of kerogen releasing oxygen-containing groups), and the optimum temperature for organic acid preservation is 80–120 °C. At lower temperatures, organic acids may be decomposed by bacteria. When the temperature rose to 120–160 °C, carboxylate anions were converted into hydrocarbons and CO_2 by thermal decarboxylation, raising the concentration of CO_2 in solution and reducing the concentration of organic acids. However, the presence of organic acids maintained the pH of the fluids at 5–6 during this time. When the temperature was higher than 160 °C, the organic acids were completely converted to CO_2, and the pH of the solution during this time was mainly controlled by the concentration of CO_2. During this stage, the organic matter in Es_4^x had begun to mature and released a large quantity of organic acids. The temperature range during this stage was favorable for the preservation of organic acids, which caused the pH of the formation water to become acidic. Because of the shallow burial, the development of primary porosity, and good pore connectivity, the strata also exhibited the properties of an open hydrologic system with normal fluid pressure. In this environment, feldspar dissolved to form secondary pores. This resulted in the precipitation under appropriate conditions of authigenic kaolinite and first phase quartz overgrowths. As stated above, the time of the early feldspar dissolution as determined by the homogenization temperatures of aqueous inclusions in the quartz overgrowths was approximately dated to 42 Ma before the present, which is the same as the feldspar dissolution under an organic acid environment. A study by Wang (2010) suggested that gypsum began to convert to anhydrite through dehydration as the formation temperature exceeded 90 °C, and large-scale dehydration can be expected during 100–150 °C. Thus, at approximately 42 Ma, significant amounts of gypsum started to dehydrate as the bottom temperature reached 100 °C, with a portion of OH^- and Ca^{2+} dissolving in the water from dehydration of gypsum.

However, the concentration of organic acids in the strata during this period reached a maximum, which caused the formation water to remain acidic. Under conditions of acidic formation water, Ca^{2+} does not precipitate as carbonate. As the temperature reached 100 °C, smectite gradually transformed into illite through the middle state of the mixed-layer of illite/smectite (I/S) in alkaline potassium-rich solutions (Wang 2010). Although the temperature reached the conversion temperature of smectite to I/S, and although the formation water was rich in K^+ and Al^{3+} because of feldspar dissolution, smectite was not converted to I/S because of the presence of the acidic formation water. Although secondary pores were abundant during this stage, primary pores still dominated the reservoir spaces in the SPDZs in Es_4^x because of the short dissolution time (only 3 Ma) and the development of primary pores (Fig. 6). From 41 to 24.6 Ma before the present (late depositional period of the Dongying Formation), the top boundary of the strata was buried at 3090 m at temperatures of 130 °C, and the bottom boundary was buried at 3690 m at temperatures of 150 °C. The decarboxylation of organic acids began during this period, which formed CO_2 and hydrocarbons and significantly reduced the concentration of organic acids. Gypsum entered the large-scale dehydration stage, during which the presence of alkaline water controlled the pH of the formation water. In this alkaline environment, smectite quickly transformed into I/S, which released metal ions such as Ca^{2+}, Na^+, Fe^{2+}, Mg^{2+}, and Si^{4+}. In this alkaline environment, which was rich in K^+, Fe^{2+}, and Mg^{2+}, the early kaolinite was rapidly converted to illite and chlorite. Under alkaline conditions with Ca^{2+}, Fe^{2+}, and Mg^{2+}, detrital quartz and the early stage overgrowths dissolved to form secondary pores, and significant amounts of carbonate cements precipitated to fill primary pores and early feldspar pores. The reservoirs in Es_4^x exhibit three stages of hydrocarbon accumulation. The first stage occurred from the end of the depositional period of Es_2 (or the early depositional period of Es_3^z) to the late depositional period of the Dongying Formation, from approximately 38 Ma (or 41 Ma) to 24.6 Ma before the present. The second and third stages experienced continuous charging of hydrocarbons, which occurred from the mid-late depositional period of the Guantao Formation to the present (Song et al. 2009a, b). A study by Sui et al. (2010) showed that when the nearshore subaqueous fans in the northern zone of the Minfeng Sag were buried deeper than 3200 m, the inner fan subfacies acted as lateral seals for the hydrocarbon reservoirs. Therefore, the middle fan could have formed lithologic traps because of the lateral plugging of the inner fan and the normal lacustrine mudstone seal. Thus, when the organic matter became highly mature, massive amounts of oil and gas migrated into the top part of the "fan-anticlines" and middle fan lithologic traps at depths greater than 3200 m, which formed early hydrocarbon reservoirs. A study on the evolution of formation pressure showed that this hydrocarbon charging period was accompanied by fluid overpressure, which protected the reservoir pores. The point contacts of grains and abundant primary pores can still be identified in the Fengshen1 well (Wang 2007) (Appendix Fig. 10A). Carbonate cementation was significantly inhibited in reservoirs with hydrocarbon charging, and the present reservoirs are characterized by a lower amount of euhedral carbonate cements (Appendix Fig. 10B). However, reservoirs without hydrocarbon charging were intensely filled by carbonate cements because of the long duration of the alkaline environment. A statistical analysis of the percentage of secondary pores after carbonate cementation showed that the reservoir spaces in the SPDZs were mainly primary pores, and the percentage of secondary pores was less than 15 % (Wang 2010) (Fig. 6).

The strata experienced uplift and then subsidence from 24.6 to 7 Ma before the present (the end of the depositional period of the Guantao Formation). During this period, the top boundary was uplifted to 2680 m and then subsided to 2990 m, while the bottom was uplifted to 3280 m and then subsided to 3590 m. The temperature of the top boundary fell to 110 °C and then increased to 120 °C, while the temperature of the bottom boundary fell to 135 °C and then increased to 140 °C. During this period, the organic matter stopped producing hydrocarbons, but the evolution of the organic matter still generated large amounts of organic acids, which were preserved at a favorable temperature and caused the formation water to be acidic. The tectonic movements of the Chennan Fault destroyed the initial hydrocarbon reservoirs and caused the loss of hydrocarbons and release of fluid overpressure. Meanwhile, meteoric freshwater penetrated deep formations using faults as conduits. The strata in Es_4^x were thought to have been buried relatively deeply during the uplift stage; thus, meteoric fresh water had a weak effect on reservoir reconstruction.

During this stage, the organic acids primarily reconstructed the reservoirs at the bottom of "paleo-reservoirs", which had been charged with fewer hydrocarbons, or in reservoirs where hydrocarbons had leaked. The organic acids dissolved carbonate cements and small amounts of feldspars, which caused second phase quartz overgrowths to develop in the reservoirs. This process occurred because these reservoirs were protected by overpressure and hydrocarbons, which made the early cementation relatively weak and led to higher porosity and good fluidity in these reservoirs. However, acidic fluids had difficulty in flowing into reservoirs with strong carbonate cementation, which acted as an obstacle for reservoir reconstruction and effective reservoir formation. The degree of reservoir reconstruction was limited during this stage; thus, the reservoir spaces in the secondary pore development zones were mainly primary pores (Fig. 6).

The strata subsided quickly from 7 to 2 Ma before the present (the end of the depositional period of the Minghuazhen Formation). The top boundary was buried at 3600 m, and the bottom was buried at 4200 m. The temperatures of the top and bottom boundaries were 140 and 165 °C, respectively. Organic matter reached the second hydrocarbon generation peak and produced large amounts of crude oil and associated gas. The center of the Minfeng Sag had already entered the condensate gas stage. Many organic acids began to decompose by thermal decarboxylation, which decreased the acidity of the formation water. Later, the reservoirs were mainly charged with oil and gas, which were further supplements to the "paleo-reservoirs". Li et al. (2010a, b) showed that normal pressure charging occurred during this period. When little formation water was flowing, the degree of hydrocarbon charging was limited. Thus, the oil charging during this period was only a supplement to early stage hydrocarbon reservoirs. According to Li et al. (2010a, b), the gas reservoirs in Es_4^x in the Fengshen1 well were mainly gas from oil cracking, which demonstrated that the contribution of later-stage charging to the present reservoirs was subordinate. During this period, the rocks had basically consolidated and the emplacement of hydrocarbons inhibited diagenesis, so compaction and cementation had little effect on reservoir reconstruction. At the same time, the formation temperature reached the threshold for the thermochemical sulfate reduction (TSR) reaction, and organic acids and H_2S were formed from hydrocarbon and anhydrite reactions. These acidic fluids could dissolve feldspars and carbonates, forming third phase quartz overgrowths with fluid inclusions with homogenization temperatures from 140 to 160 °C (Table 2). However, the formation was a relatively closed geochemical system during this period, and large amounts of water flow and material transport were impossible, so the amount of acidic fluids from the TSR reaction and the amount of secondary pores from the dissolution of feldspar and carbonate were small. Therefore, primary pores still dominated in the reservoirs in the SPDZs (Fig. 6).

From 2 Ma to the present, the top boundary of the strata was buried at 3890 m at temperatures of 150 °C, and the bottom boundary was buried at 4490 m at temperatures of 170 °C. During this stage, the organic acids had almost been completely decomposed, which caused the formation water to be weakly acidic with a pH of 6–7. Organic matter began generating condensate gas, and crude oil in the "paleo-reservoirs" started to crack and form large amounts of asphalt and H_2S. The TSR reactions also produced some H_2S. Later pyrite from the reaction between H_2S and Fe^{2+} in the reservoirs replaced the initial cements and filled the pores. Evidence of petroleum cracking in the "paleo-reservoirs" was discussed in detail as part of the diagenetic evolution sequence. The later cementation of asphalt and pyrite destroyed a large amount of primary porosity in the "paleo-reservoirs", which caused the proportion of secondary pores to exceed that of primary pores (Fig. 2, Fig. 6). According to the definition of the SPDZ, the SPDZs in Es_4^x in the northern zone of the Minfeng Sag formed when many primary pores were filled with asphalt and pyrite from oil cracking since 2 Ma.

6 Conclusions

(1) Secondary pore development zones can be defined in three ways: (1) the percent of secondary pores is greater than 50 %; (2) the porosity of the reservoirs is higher than the effective reservoir porosity cutoff because the absolute content of secondary pores is high; and (3) high porosity reservoirs concentrate to form belts at particular depth intervals in the porosity-depth profile, with the porosity envelope curve bulging toward higher porosities. Accordingly, two secondary pore development zones exist in Es_4^x in the northern zone of the Minfeng Sag, which range from 4200 to 4500 m and from 4700 to 4900 m.

(2) The secondary pore development zones in Es_4^x in the northern zone of the Minfeng Sag experienced the following processes. Significant numbers of secondary pores (although fewer than primary pores) formed from the dissolution of feldspar in an early organic acid environment. During this stage, the burial depth of the reservoirs was shallow. The pore spaces were slightly changed during strata subsidence—uplift—subsidence because of early hydrocarbon charging and overpressure protection. Finally, the present secondary pore development zones formed when many primary pores were filled by massive asphalt and pyrite from oil cracking in deeply buried paleo-reservoirs.

Acknowledgments The research is co-funded by National Natural Science Foundation of China (Grant No. 41102058, Grant No. U1262203, and Grant No. 41202075), the National Science and Technology Special Grant (Grant No. 2011ZX05006-003), the Fundamental Research Funds for the Central Universities (Grant No. 14CX02181A, Grant No. 15CX08001A, and Grant No. 15CX0 5007A), and Shandong Natural Science Foundation (Grant No. ZR2011DQ017). The authors thank the Geological Scientific Research Institute of Sinopec Shengli Oilfield Company, the Exploration and Development Research Institute of Sinopec Zhongyuan Oilfield Company, and the CNPC key laboratory of oil and gas reservoirs in China University of Petroleum for providing database and technological assistance.

Appendix 1

See Appendix Fig. 7.

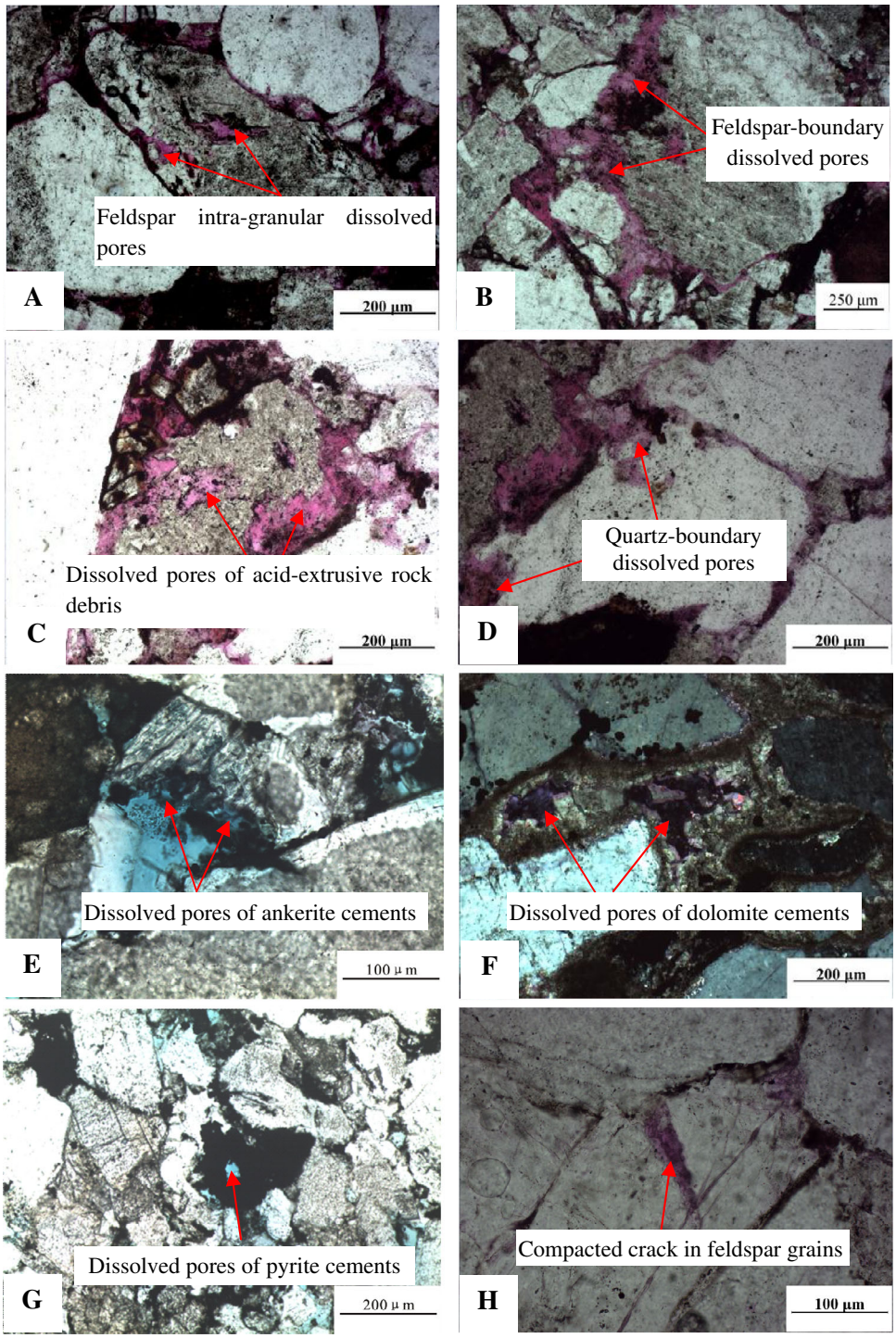

Fig. 7 **A** Fengshen1 well, 4321.9 m, intra-granular-dissolved pores in feldspar grains. **B** Fengshen1 well, 4321.9 m, dissolved pores along feldspar grain boundaries. **C** Fengshen1 well, 4321.9 m, dissolved pores in acid extrusive rock debris. **D** Fengshen1 well, 4321.9 m, dissolved pores along quartz grain boundaries. **E** Fengshen1 well, 4323.3 m, dissolved pores in ankerite cement. **F** Fengshen4 well, 4476.15 m, dissolved pores in dolomite cement. **G** Fengshen1 well, 4348.25 m, dissolved pores in pyrite cement. **H** Fengshen3 well, 4867 m, compacted cracks in feldspar grains

Appendix 2

See Appendix Fig. 8.

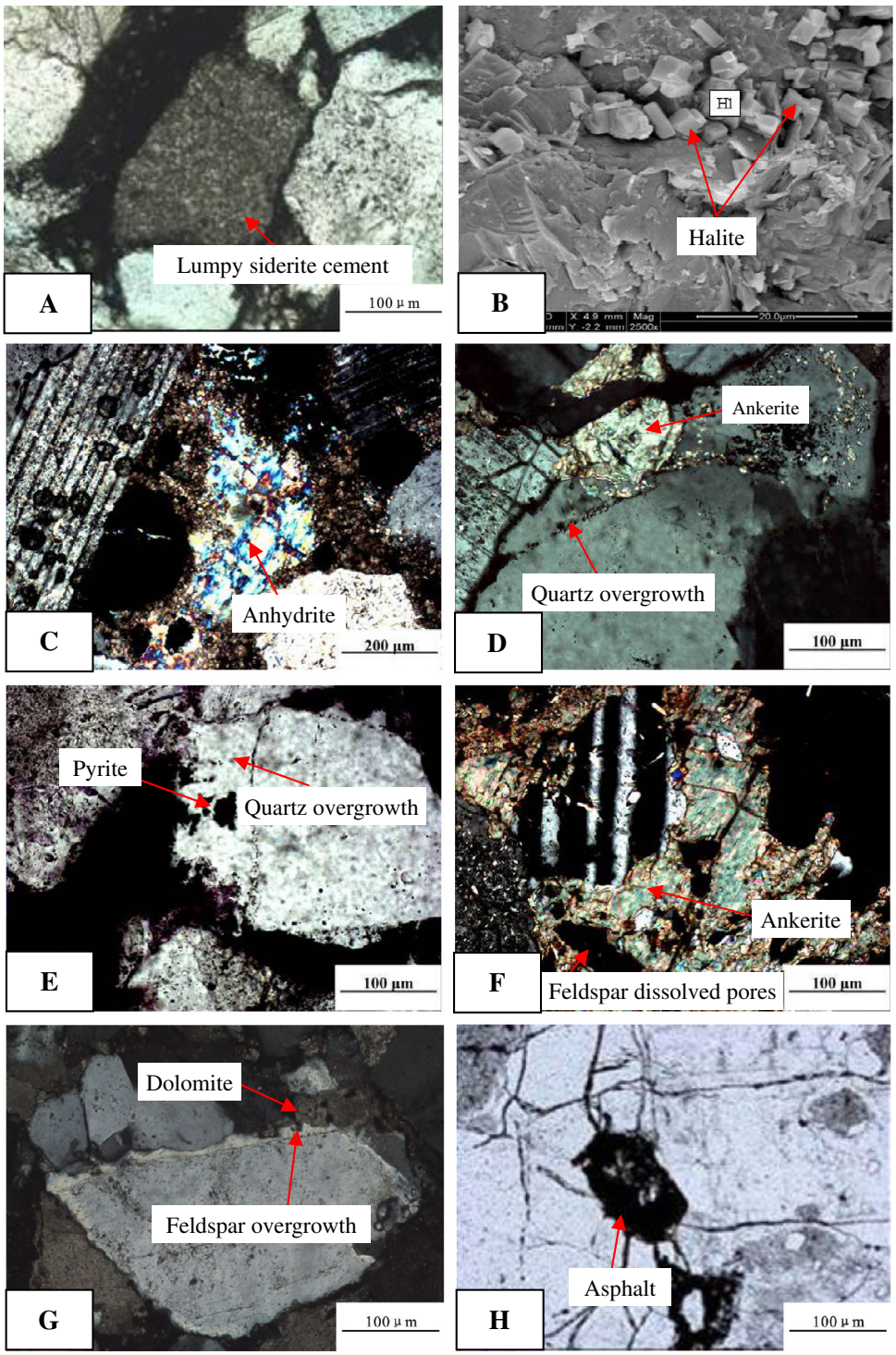

Fig. 8 **A** Fengshen1 well, 4323.3 m, lumpy siderite cement. **B** Feng8 well, 4397.15 m, halite-filled pores (SEM). **C** Feng8 well, 4397.15 m, anhydrite that replaced ankerite. **D** Fengshen3 well, 4867 m, ankerite that replaced quartz overgrowths. **E** Fengshen3 well, 4867 m, pyrite that replaced quartz overgrowths. **F** Fengshen3 well, 4867 m, ankerite filling parts of the feldspar-dissolved pores. **G** Fengshen1 well, 4350 m, dolomite that replaced feldspar overgrowths. **H** Fengshen1 well, 4321.9 m, asphalt filling intra-granular-dissolved pores in feldspar grains (Li et al. 2010a, b)

Appendix 3

See Appendix Fig. 9.

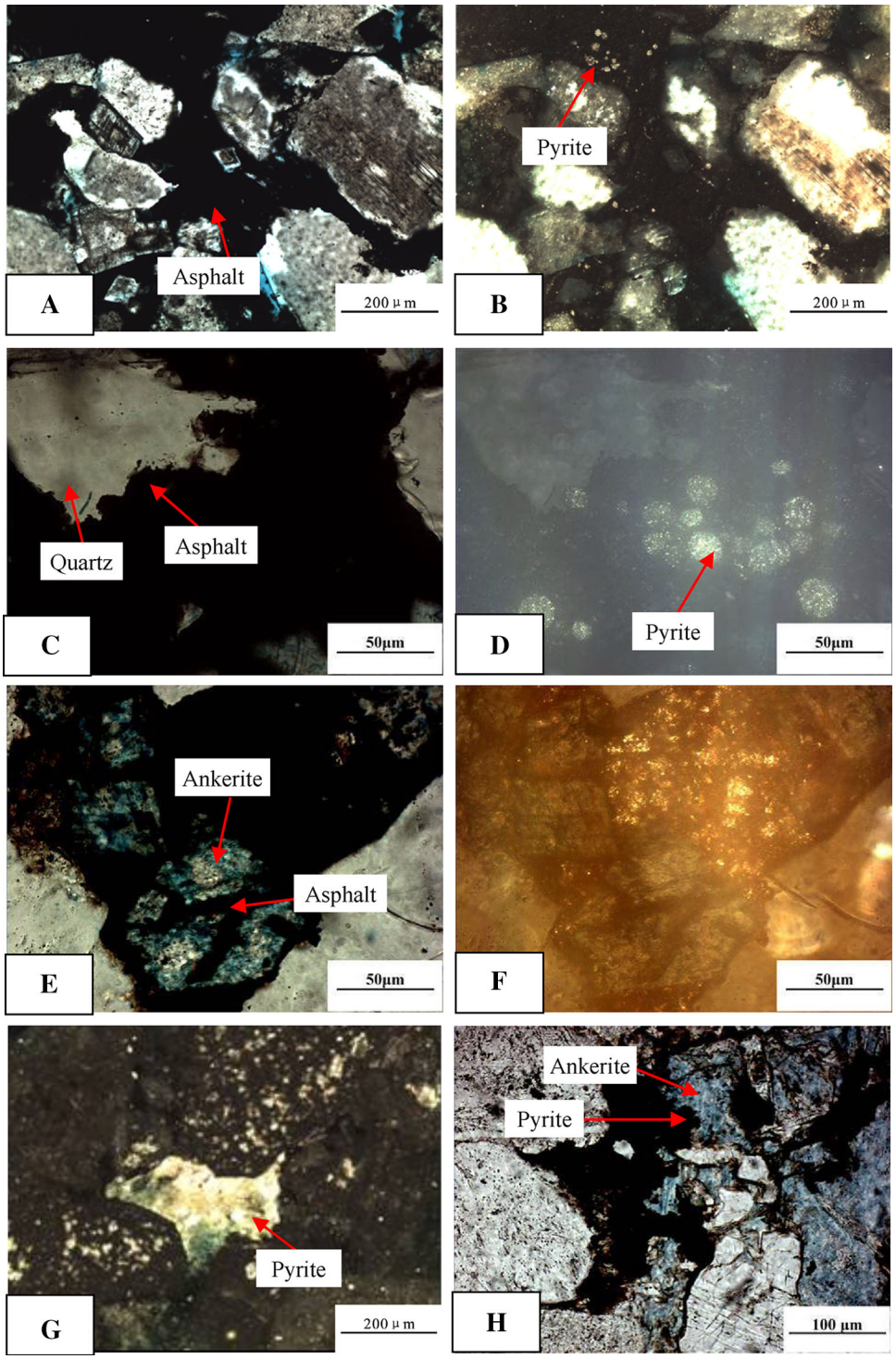

Fig. 9 **A** Fengshen1 well, 4323.3 m, asphalt and star-like pyrite filling intergranular pores. **B** Fengshen1 well, 4323.3 m, reflected light, the same visual area as A. **C** Fengshen1 well, 4321.9 m, asphalt and pyrite filling quartz-dissolved pores. **D** Fengshen1 well, 4321.9 m, reflected light, the same visual area as C. **E** Fengshen1 well, 4321.9 m, asphalt filling dissolved pores in ankerite cement. **F** Fengshen1 well, 4321.9 m, reflected light, the same visual area as E. **G** Fengshen1 well, 4323.3 m, reflected light, pyrite cement. **H** Fengshen3 well, 4867 m, pyrite that replaced ankerite

Appendix 4

See Appendix Fig. 10.

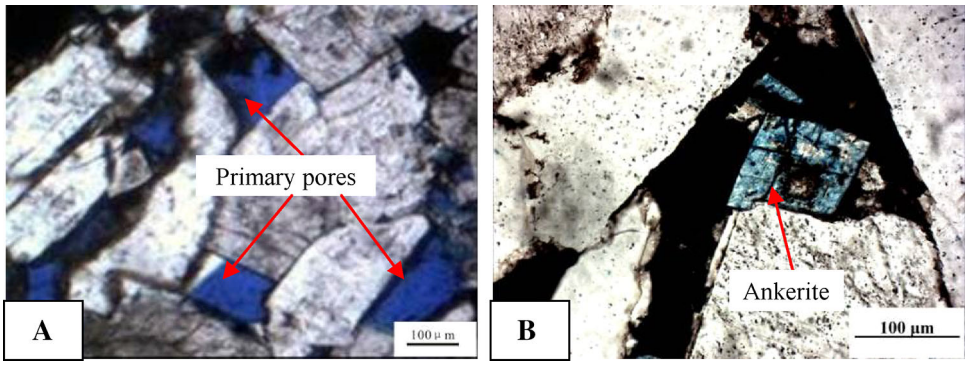

Fig. 10 **A** Fengshen1 well, 4322.5 m, primary pores (Wang 2010). **B** Fengshen1 well, 4321.9 m, complete crystal ankerite filling intergranular pores

References

Ajdukiewicz JM, Larese RE. How clay grain coats inhibit quartz cement and preserve porosity in deeply buried sandstones: observations and experiments. AAPG Bulletin. 2012; 96(11):2091–119.

Bjørlykke K, Jahren J. Open or closed geochemical systems during diagenesis in sedimentary basins: constraints on mass transfer during diagenesis and the prediction of porosity in sandstone and carbonate reservoirs. AAPG Bulletin. 2012;96(12): 2193–214.

Bjørlykke K. Relationships between depositional environments, burial history and rock properties: some principal aspects of diagenetic process in sedimentary basins. Sed Geol. 2014;301: 1–14.

Bloch S, Lander RH, Bonnell L. Anomalously high porosity and permeability in deeply buried sandstone reservoirs: origin and predictability. AAPG Bulletin. 2002;86:301–28.

Cao YC, Yuan GH, Li XY, et al. Characteristics and origin of abnormally high porosity zones in buried Paleogene clastic reservoirs in the Shengtuo area, Dongying Sag, East China. Pet Sci. 2014;11:346–62.

Curtis CD. Possible links between sandstone diagenesis and depth-related geochemical reactions occurring in enclosing mudstones. J Geolog Soc. 1978;135:107–17.

Dutton SP, Loucks RG. Diagenetic controls on evolution of porosity and permeability in Lower Tertiary Wilcox sandstones from shallow to ultradeep (200–6700 m) burial, Gulf of Mexico Basin, U.S.A. Mar Pet Geol. 2010;27(1):69–81.

Ehrenberg SN. Preservation of anomalously high porosity in deeply buried sandstones by grain-coating chlorite: examples from the Norwegian Continental Shelf. AAPG Bull. 1993;77:1260–86.

Giles MR, De Boer RB. Origin and significance of redistributional secondary porosity. Mar Pet Geol. 1990;7:378–97.

Higgs KH, Zwingmann H, Reyes AR, et al. Diagenesis, porosity evolution, and petroleum emplacement in tight gas reservoirs, Taranaki Basin, New Zealand. J Sediment Res. 2007;77: 1003–25.

Hu WR, Bao JW, Hu B. Trend and progress in global oil and gas exploration. Pet Explor Dev. 2013;40(4):409–13 **(in Chinese)**.

Jiang ZX, Qiu LW, Chen GJ. Alkaline diagenesis and its genetic mechanism in the Triassic coal measure strata in the Western Sichuan Foreland Basin, China. Pet Sci. 2009;6(4):354–65.

Li CQ, Chen HH, Liu HM. Identification of hydrocarbon charging events by using micro-beam fluorescence spectra of petroleum inclusions. Earth Sci. 2010a;35(4):657–62 **(in Chinese)**.

Li YJ, Song GQ, Li WT, et al. A fossil oil-reservoir and the gas origin in the Lower Sha-4 Member of the well Fengshen-1 area, the north Dongying Zone of the Jiyang Depression. Oil Gas Geol. 2010b;31(2):173–9 **(in Chinese)**.

Liu H, Jiang ZX, Zhang RF, et al. Gravels in the Daxing conglomerate and their effect on reservoirs in the Oligocene Langgu Depression of the Bohai Bay Basin, North China. Mar Pet Geol. 2012;29:192–203.

Liu W, Zhu XM. Distribution and genesis of secondary pores in Tertiary clastic reservoir in southwestern Qaidam Basin. Pet Explor Dev. 2006;33(3):315–8 **(in Chinese)**.

Liu YX, Zhu M, Zhang SM. Diagenesis and pore evolution of reservoir of the Member4 of Lower Cretaceous Quantou Formation in Sanzhao Sag, northern Songliao Basin. J Palaeogeogr. 2010;12(4):480–7 **(in Chinese)**.

Ma WM, Wang XL, Ren LY. Overpressure and secondary pores in Dongpu Depression. J Northwest Univ (Nat Sci Edition). 2005;35(3):325–30 **(in Chinese)**.

Meng YL, Liang HW, Meng FJ, et al. Distribution and genesis of the anomalously high porosity zones in the middle-shallow horizons of the Songliao Basin. Pet Sci. 2010;7(3):302–10.

Meng YL, Liu WH, Meng FJ, et al. Distribution and origin of anomalously high porosity zones of the Xujiaweizi Fault Depression in Songliao Basin. J Palaeogeogr. 2011;13(1):75–84 **(in Chinese)**.

Osborne MJ, Swarbrick RE. Diagenesis in North Sea HPHT clastic reservoirs—consequences for porosity and overpressure prediction. Mar Pet Geol. 1999;16:337–53.

Qiu LW, Jiang ZX. Alkaline diagenesis of Terrigenous clastic rocks. Beijing: Geological Publishing Press; 2006. p. 22 **(in Chinese)**.

Schmidt V, McDonald DA. Role of secondary porosity in sandstone diagenesis. AAPG Bull. 1977;61:1390–1.

Schmidt V, McDonald D. A texture and recognition of secondary porosity in sandstones. Special Publication. Soc Econ Paleontol Mineral, 1979;26:209–225.

Shi ZF, Zhang ZC, Ye SD. The mechanism of secondary pores in the reservoir of Funing Formation in Gaoyou Depression of Subei Basin. Acta Sedimentol Sin. 2005;23(3):429–36 **(in Chinese)**.

Song GQ, Jiang YL, Liu H, et al. Pooling history of cracked gas in middle-deep reservoirs in Lijin-Minfeng areas of the Dongying Sag. Nat Gas Ind. 2009a;29(4):14–7 **(in Chinese)**.

Song GQ, Jin Q, Wang L. Study on kinetics for generating natural gas of Shahejie Formation in deep-buried sags of Dongying Depression. Acta Pet Sinica. 2009b;33(5):672–7 **(in Chinese)**.

Sui FG, Cao YC, Liu HM. Physical properties evolution and hydrocarbon accumulation of Paleogene nearshore subaqueous fan in the eastern north margin of the Dongying Depression. Acta Geol Sinica. 2010;84(2):246–56 **(in Chinese)**.

Sun LD, Fang CL, Li F, et al. Innovations and challenges of sedimentology in oil and gas exploration and development. Pet Explor Dev. 2015;42(2):129–36 **(in Chinese)**.

Sun LD, Zou CN, Zhu RK, et al. Formation, distribution and potential of deep hydrocarbon resources in China. Pet Explor Dev. 2013;40(6):641–9 **(in Chinese)**.

Surdam RC, Boese SW, Crossey GJ. The chemistry of secondary porosity. AAPG Memoir. 1984;37:127–51.

Surdam RC, Crossey LJ, Hagen ES, et al. Organic-inorganic interactions and sandstone diagenesis. AAPG Bull. 1989;73:1–23.

Taylor TR, Giles MR, Hathon LA, et al. Sandstone diagenesis and reservoir quality prediction: models, myths, and reality. AAPG Bull. 2010;94:1093–132.

Taylor TR, Kittridge MG, Winefield P, et al. Reservoir quality and rock properties modeling—Triassic and Jurassic sandstones, Greater Shearwater Area, UK Central North Sea. Mar Pet Geol. 2015;65:1–21.

Wang P, Zhao CL. An approach to the generating mechanism of secondary pores in Duqiaobai area of Dongpu Depression. Pet Explor Dev. 2001;28(4):44–6 **(in Chinese)**.

Wang SP. Diagenesis researches of natural gas reservoir with gyprock and salt bed in Minfeng area of the lower part of Number4 of Shahejie Formation in Dongying Depression. Master's Thesis. China University of Petroleum. 2007 (in Chinese).

Wang YZ. Genetic mechanism and evolution model of secondary pore development zone of Paleogene in the north zone in Dongying Depression. Ph. D. Thesis. China University of Petroleum. 2010 (in Chinese).

Wang YZ, Cao YC, Ma BB, et al. Mechanism of diagenetic trap formation in nearshore subaqueous fans on steep rift lacustrine basin slopes—a case study from the Shahejie Formation on the north slope of the Minfeng Subsag, Bohai Basin, China. Pet Sci. 2014;11:481–94.

Wang ZG. Pooling model of steep slope structure and lithological zone in north Dongying Sag. Pet Explor Dev. 2003;20(4):10–2 **(in Chinese)**.

Wang ZY, Wang FP, Lin XY. Pore types and origin of secondary pores of Triassic and Jurassic in north Tarim. Oil Gas Geol. 1995;16(3):203–10 **(in Chinese)**.

Warren EA, Pulham AJ. Anomalous porosity and permeability preservation in deeply buried Tertiary and Mesozoic sandstones in the Cusiana field, Llanos Foothills, Colombia. J Sediment Res. 2001;71(1):2–14.

Wilkinson M, Haszeldine RS. Oil charge preserves exceptional porosity in deeply buried, overpressured sandstones: Central North Sea, UK. J Geolog Soc. 2011;168:1285–95.

Yuan GH, Gluyas J, Cao YC, et al. Diagenesis and reservoir quality evolution of the Eocene sandstones in the northern Dongying Sag, Bohai Bay Basin, East China. Mar Pet Geol. 2015;62:77–89.

Yuan J, Wang ZQ. Distribution and generation of deep reservoir secondary pores, Paleogene, Dongying Sag. J Mineral Pet. 2001;21(1):43–7 **(in Chinese)**.

Zeng JH. Effect of fluid-rock interaction on porosity of reservoir rocks in Tertiary system, Dongying Sag. Acta Pet Sinica. 2001;22(4):39–43 **(in Chinese)**.

Zhang Q, Zhong DK, Zhu XM. Pore evolution and genesis of secondary pores in Paleogene clastic reservoirs in Dongying Sag. Oil Gas Geol. 2003;24(3):281–5 **(in Chinese)**.

Zhang Q, Zhu XM, Steel RJ, et al. Variation and mechanisms of clastic reservoir quality in the Paleogene Shahejie Formation of the Dongying Sag, Bohai Bay Basin, China. Pet Sci. 2014;11:200–10.

Zhang SW. "Water consumption" in diagenetic stage and its petroleum geological significance. Acta Sedimentol Sin. 2007;25(5):701–7 **(in Chinese)**.

Zhang WC, Li H, Li HJ. Genesis and distribution of secondary porosity in the deep horizon of Gaoliu area, Nanpu Sag. Pet Explor Dev. 2008;35(3):308–12 **(in Chinese)**.

Zhang YG, Xu WP, Wang GL. Hydrocarbon Reservoir Formation Aggregation in a Continental Rift Basin, East China. Beijing: Petroleum Industry Press; 2006. p. 127–31 **(in Chinese)**.

Zheng MY, Wu RL. Diagenesis and pore zonation of sandstone reservoirs in Huanghua Depression. Oil Gas Geol. 1996;17(4):268–75 **(in Chinese)**.

Zhong DK, Zhu XM, Zhang ZH. Origin of secondary porosity of Paleogene sandstone in the Dongying Sag. Pet Explor Dev. 2003;30(6):51–3 **(in Chinese)**.

Zhong JH, Wang GZ, Gao XC. Sedimentary features, genesis and relation to hydrocarbon of fan-anticline in the north slope of the Dongying Sag. Chin J Geol (Scientia Geologica Sinica). 2004;3(4):625–36 **(in Chinese)**.

Zhu SF, Zhu XM, Wang YB. Dissolution characteristics and pore evolution of Triassic reservoir in Ke-Bai area, northwestern margin of Junggar Basin. Acta Sediment Sin. 2010;28(3):548–54 **(in Chinese)**.

Zhu XM, Mi LJ, Zhong DK. Paleogene diagenesis and its control on reservoir quality in Jiyang Depression. J Palaeogeogr. 2006;8(3):296–305 **(in Chinese)**.

Zhu XM, Wang YG, Zhong DK. Pore types and secondary pore evolution of Paleogene reservoir in the Jiyang Sag. Acta Geol Sinica. 2007;81(2):197–204 **(in Chinese)**.